Thesis for the Degree of Master of Science

A Numerical study on flow and dispersion in an urban area using a CFD/WRF coupled model

by

Jae-Won Choi

Department of Environmental Atmospheric Sciences

The Graduate School

Pukyong National University

August 2010

A Numerical study on flow and dispersion in an urban area using a CFD/WRF coupled model

CFD-WRF 접합모델을 이용한 도시지역 흐름과 확산 연구

Advisor: Prof. Jae Jin Kim

by
Jae-Won Choi

A thesis submitted in partial fulfillment of the requirements
for the degree of

Master of Science

in Department of Environmental Atmospheric Sciences, the Graduate School,
Pukyong National University

August 2010

A Numerical study on flow and dispersion in an urban area using a CFD/WRF coupled model

A dissertation

by

Jae-Won Choi

Approved by:

(Chairman) Hyeong-Bin Cheong

(Member) Byung-Hyuk Kwon

(Member) Jae-Jin Kim

August 2010

CONTENTS

List of Figures iii
List of Tables iv
Abstract vii
1. Introduction 1
2. Numerical Experiment 5
  2.1 CFD model 5
  2.2 WRF model 8
  2.3 Experimental setup 10
    a. Mesoscale model 10
    b. CFD model 12
  2.4 Coupling method 17
3. Result and discussion 20
  3.1 Verification of result of a WRF model 20
  3.2 Simulation with a coupled CFD-WRF model 28
4. Summary and conclusions 31

References 34

LIST OF FIGURES

Fig. 1 Representation of model domains in the WRF simulation 11

Fig. 2 (a) A picture of Konkuk university area and (b) building configuration in the CFD model domain...................................... 13

Fig. 3 The schematic process of constructing model domain for a CFD using a GIS data... 14

Fig. 4 Simulated area (yellow broken line) and interest area (yellow solid line) 16

Fig. 5 The grid structure in WRF and CFD model 19

Fig. 6 (a) Simulated sea-level pressure field at 00 UTC 10 January 2009 and (b) Observed sea-level pressure field at 00 UTC 10 January 2009 from KMA weather chart 21

Fig. 7 (a) Simulated sea-level pressure field at 00 UTC 11 January 2009 and (b) Observed sea-level pressure field at 00 UTC 11 January 2009 from KMA weather chart 22

Fig. 8 Time series of simulated and observed temperature at z = 52m 25

Fig. 9 Time series of simulated and observed wind direction at z = 52m 26

Fig. 10 Time series of simulated and observed wind speed at z = 52m . 27

LIST OF TABLES

Table 1. Experimental design in the WRF simulation. 9

Table 2. Mean error and correlation of wind speeds simulated in WRF and CFD-WRF model to observed wind speeds in AWS 30

A Numerical study on flow and dispersion in an urban area using a CFD/WRF coupled model

Jae-Won Choi

Department of Environmental Atmospheric Sciences, The Graduate School, Pukyong National University

Abstract

This study, examined the effects of highly developed residential buildings on wind flow and pollutant dispersion in a built-up area of Seoul, South Korea. Predicting realistic flows in an urban area, it is very important to reflect variations of a mesoscale weather field. For this, a mesoscale numerical weather prediction model, the Weather Research and Forecasting (WRF) model is employed and coupled with a computational fluid dynamics (CFD) model. The CFD model is based on a Reynolds-averaged Navier-Stokes equations model with the renormalization group (RNG) turbulence closure scheme. Output data sets produced by the WRF model which can simulate mesoscale weather well are used as the initial input data sets in the CFD model. The CFD model is numerically integrated using the data sets which are properly interpolated in time and space. The WRF model is simulated for 30 hours starting from 18 UTC 9 January 2009 using NCEP final analysis data as initial and boundary conditions. During the period, a high-pressure system was dominant, clear condition is maintained, and synoptic winds are weak. Four nested computational domains are considered and grid sizes of the innermost domain are 1km in the horizontal. The coupled CFD-WRF model is integrated for 24 hours. Sea level

pressures are well reproduced during the simulation period by WRF model compared with the analysis charts. The results showed the importance of the coupled CFD-WRF model in predicting the wind speed and direction in urban areas. The CFD-WRF model predicted them better than those by the WRF model alone. It is because the CFD-WRF model considered adjacent buildings and more realistic topographies. The results also showed that tall buildings in the urban area affected the flow and pollutant dispersion much in the domain. The pollutant concentration inside the area bounded by the tall buildings is low due to the partial increase in the wind speed (so called, the channeling effect) even though the area is near from the pollutant sources.

1. Introduction

As the industrial structure changed from the secondary industry which is divided into industrial and residential areas to the tertiary industry, both areas have been located in urban area as a unified form. Therefore the majority of the population is concentrated in a limited space and a shortage of various additional facilities has been occurred because of a settled population growth. Recently nearly 300 cities have a million or more inhabitants. The ratio of population in urban areas throughout the world was 13% in 1900's, 29% in 1950's and had been occupied about 49% in 2005. Furthermore, urban population is about 4.9 billions, 60% of the world's total population. To overcome these kind of problem, high rise residential buildings reached dozens to hundreds of meters have been constructed.

In urban area, one of main factors that determine the flow field is geometrical factor. The geometrical factors include the building shape and orientation and the aspect ratio, which is defined as a ratio of the building height to the width between buildings. Buildings act on inflow as on of the most important external factors. According to the building structure, arrangement and size, complicated flow field can be appeared in urban areas. For instance, wind speed will be increased at flow convergence areas between buildings and opposite phenomenon will be occured behind of them by blocking effects. Both phenomena have negative effects on inhabitants. Hazardous articles rapidly spread to adjoining areas when biochemical terrorist activities or fire accidents in downtown areas happen as wind speed increase. Yellow dust or pollutants could be congested as wind speed decrease. Therefore, the research of urban meteorological environment characteristics is very important, which makes it possible to alleviate the increasingly serious urban environmental problems. The most important features of street canyon (relatively narrow street in-between buildings that line up continuously along both sides) micro climate are the wind-induced flow patterns, such as air recirculation. These unique microscale meteorological processes not only affect the local air quality but also the comfort of the city inhabitants (Bottema, 1993).

There are quite a number of studies dedicated to street canyon through field experiments (DePaul and Sheih, 1986; Nakamura and Oke, 1988; Rotach, 1995; Eliasson et al., 2006), physical experiments (Meroney et al., 1996; Baik et al., 2000; Brown et al., 2000; Uehara et al., 2000), and numerical experiments (Lee and Park, 1994; Sini et al., 1996; Baik and Kim, 1999; Kim and Baik, 1999, 2001; Liu and Barth, 2002; Cheng and Hu, 2005). Field experiments provide most realistic results because it is carried out in a real-world and reflects all of dominant parameterizations, e.g. building influences and meteorological conditions. However, the high cost makes it difficult to apply broad scale experiments and it also hard to clearly investigate which parameter affects on observed values. Physical experiments have a strong point that could identify parameters which affect on experiments as it performed using a scaled model but it has same problem that the filed experiment has. On the contrary, numerical experiments could apply various physical conditions by low cost and are possible to repeated simulation and predicting flow patterns. With the ever-increasing computational power, CFD models which commonly used for numerical experiments have become a useful tool to explain the processes occurring in street canyons. Moreover, it has been possible to rapidly and accuaratealy make 3D geographical domain using a Geographical Information System (GIS) data which has informations of height and position of buildings. Thus, many studies are proceeded using a CFD model with a model domain constructed by a GIS data. (Chu et al., 2005)

With the continuous development of urbanization, the research on meteorological environment in a single-scale model is not able to satisfy the requirements of city developments. Numerical model can apply meteorological conditions using a mesoscale model which can predict weather condition.

In this study, model domain is constructed using a GIS data and CFD model with RNG k-e turbulence model is used to simulate flow and scala dispersion in urban area (Kim and Baik, 2005). A flow formed in a microscale area is dominated by mesoscale weather phenomena like a valley wind or a see-breeze. So, it is necessary to consider a mesoscale or a regional scale weather phenomena to obtain more realistic flow and dispersion.

Flow which forms a microscale region is influenced by a mesoscale and a regional scale meteorological conditions. Therefore, it is necessary to consider such meteorological conditions to simulate realistic flow and dispersion at urban areas. For this, there are great concern on coupling a microscale model with a mesoscale model (Baik et al., 2000).

In the present study, we investigated flow characteristics of flow and dispersion around the Konkuk university coupling a Computational Fluid Dynamics (CFD) model which can simulate flow in a micro scale with a Weather Research and Forecasting (WRF) model which is used widely for predicting a mesoscale weather phenomena. For this, simulated data with a WRF model are used to initial boundary conditions for a CFD model.

2. Numerical experiment setup

2.1 Computational Fluid Dynamics model

As a CFD model, the Reynolds-averaged Naver - Stokes equations model with the renormalization group (RNG) $k-\epsilon$ turbulence model developed by Kim and Baik (2004) is used in this study. The CFD model assumes three dimentional, non hydrological, uncompressible flow system and excludes coriolis force. Reynolds averaged momentum equation, mass conservation equation and scalar transport equation defined as

$$\frac{\partial U_i}{\partial t} + U_j \frac{\partial U_i}{\partial x_j} = -\frac{1}{\rho_0}\frac{\partial P^*}{\partial x_i} + \nu \frac{\partial^2 U_i}{\partial x_j \partial x_j} - \frac{\partial}{\partial x_j}(\overline{u_i u_j}), \qquad (1)$$

$$\frac{\partial U_j}{\partial x_j} = 0, \qquad (2)$$

$$\frac{\partial C}{\partial t} + U_j \frac{\partial C}{\partial x_j} = D\frac{\partial^2 C}{\partial x_j \partial x_j} - \frac{\partial}{\partial x_j}(\overline{cu_j}) + S_c. \qquad (3)$$

where U_i is a component of averaged speed for i direction, t means time, x_i is i-th value in Cartesian coordinates , P^* is a pressure deviation for reference value and C represents average concentration of scalar materials. u_i is the fluctuation from U_i, c is the fluctuation from C, ρ_0 is the air density, ν is the kinematic viscosity of air, and S_c in (3) denotes the source term of pollutant. The Reynolds stress in (1) are parameterized using

$$-\overline{u_i u_j} = K_m\left(\frac{\partial U_i}{\partial x_j}+\frac{\partial U_j}{\partial x_i}\right)-\frac{2}{3}\delta_{ij}k, \tag{4}$$

Here, K_m is the eddy (or turbulent) viscosity of momentum, k is the turbulent kinetic energy, and δ_{ij} is the Kronecker delta. In the RNG $k-\epsilon$ turbulence model, K_m is represented by

$$K_m = C_\mu \frac{k^2}{\varepsilon} \tag{5}$$

where $C_\mu(=0.0845)$ is an empirical constant and ϵ is the dissipation rate of turbulent kinetic energy. Note that K_m in the RNG $k-\epsilon$ turbulence model also includes molecular kinematic viscosity. It is calculated using k and ϵ that are prognostically computed with the equations of turbulent kinetic energy and its dissipation rate, given by

$$\frac{\partial k}{\partial t}+U_j\frac{\partial k}{\partial x_j}=-\overline{u_i u_j}\frac{\partial U_i}{\partial x_j}+\frac{\partial}{\partial x_j}\left(\nu+\frac{K_m}{\sigma_k}\frac{\partial k}{\partial x_j}\right)-\varepsilon \tag{6}$$

$$\begin{aligned}&\frac{\partial \varepsilon}{\partial t}+U_j\frac{\partial \varepsilon}{\partial x_j}=\\&-C_{\varepsilon 1}\frac{\varepsilon}{k}\overline{u_i u_j}\frac{\partial U_i}{\partial x_j}+\frac{\partial}{\partial x_j}\left(\nu+\frac{K_m}{\sigma_\varepsilon}\frac{\partial \varepsilon}{\partial x_j}\right)-C_{\varepsilon 2}\frac{\varepsilon^2}{k}-R\end{aligned} \tag{7}$$

where $\sigma_k(=0.7179)$, $\sigma_\varepsilon(=0.7179)$, $C_{\varepsilon 1}(=1.42)$ and $C_{\varepsilon 2}(=1.68)$ are empirical constants. The term R in (7) is included to account for nonequilibrium strain rates in the RNG $k-\epsilon$ turbulence model are specified following Yakhot et al. (1992) and Kim and Baik (2004).

$$R=\frac{C_\mu \eta^3(1-\eta/\eta_0)\varepsilon^2}{(1+\beta_0\eta^3)k}, \tag{8}$$

$$\eta=\frac{k}{\varepsilon}\left[\left(\frac{\partial U_i}{\partial x_j}+\frac{\partial U_j}{\partial x_i}\right)\frac{\partial U_i}{\partial x_j}\right]^{1/2}. \tag{9}$$

where $\beta_0(=0.012)$ and $\eta_0(=4.377)$ are empirical constants. The above governing equation set is solved numerically on a staggered grid system using the finite-volume method following the Semi-Implicit Method for Pressure-Linked Equation (SIMPLE) algorithm.

2.2 WRF model

As a mesoscale model, a compressible, non-hydrostatic, model developed at the National Center for Atmospheric Research (NCAR) is used in this study. This model, called WRF, has been extensively and successfully used for atmospheric environmental applications as well as weather research and forecasting. WRF provides many selective parameterization options for physical processes. Table 1 shows an experimental setup applied in WRF model and several physical processes. In the present simulation using the WRF, version 3.2, microphysics is represented with a WRF Single-Moment 6-class method which is suitable for a high resolution numerical simulation and radiative processes are presented with the Rapid Radiative Transfer Model for a longwave radiation and Dudhia scheme for a shortwave radiation. Surface layer physics processes are represented with Eta similarity which based on Monin-Obukhov with Zilitinkevich thermal roughness length and standard similarity functions and Noah Land Surface Model is used for a land surface physics. To reflect roughness effect by roof top, wall and road Urban Canopy model is applied and planerary boundary layer processes are represented with the Mellor-Yamada-Janjic scheme that calculates turbulent kinetic energy prognostically. Cloud processes are represented with the New Grell scheme.

Table 1. Experimental design in the WRF simulation.

	Domain 1	Domain 2	Domain 3	Domain 4
Horizontal grid dimension	121 × 121	121 × 121	121 × 121	121 × 121
Vertical layers	21 (eta level)			
Horizontal grid size (km)	27	9	3	1
Time integration (hour)	72	24	8	2
Microphysics	WSM 6-class graupel scheme			
Longwave radiation	Rapid Radiative Transfer Model (RRTM)			
Shortwave radiation	Dudhia scheme			
Surface layer	Monin-Obukhov (Janjic Eta) scheme			
Boundary layer	Mellor-Yamada-Janjic (Eta) TKE scheme			
Cumulus option	New Grell scheme (G3)		none	
Initial/boundary conditions	NCEP final analysis data (6-h intervals, 1° × 1° resolution)			

2.3. Experimental setup

a. Mesoscale model

Figure 1 shows the computational domain used in a mesoscale model. In the WRF simulation, four one-way nested computational domains are considered with horizontal grid intervals of 27, 9, 3, and 1 km and respective time intervals of 72, 24, 8 and 2 s. The innermost domain covers the Seoul area with the Konkuk university as the center. In each of the four domains, the horizontal grid dimension is 121 × 121. There are 21 vertical layers in all of the domain. The outmost WRF domain is set up 3510km in each direction to include an air mass which affects around Korean peninsula and the innermost domain is 130km by 130km in order to reflect effect of topographies which affect an interest area. The WRF model is integrated for 30 hours starting from 00 UTC 3 August in 2006 including spin-up time for 6 hours. The National Centers for Environmental Prediction (NCEP) final analysis data, which are in 6 hours intervals and have a horizontal resolution of 1° × 1°, are used as initial and boundary conditions in the WRF simulation.

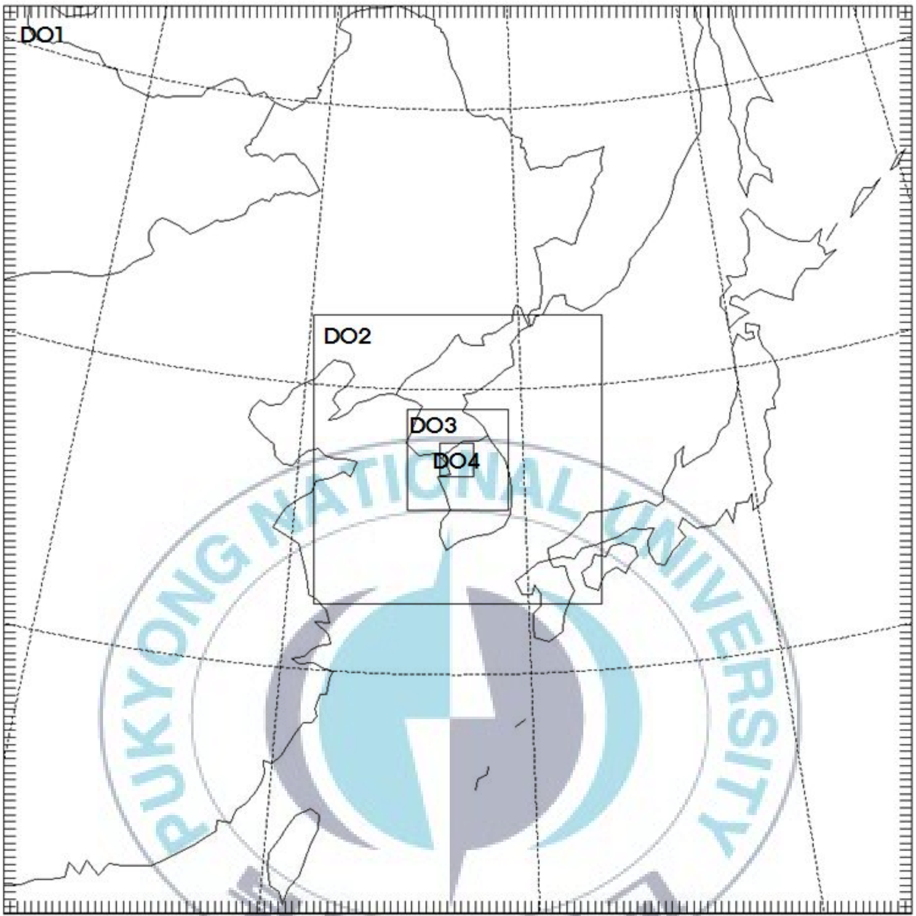

Fig. 1. Representation of model domains in the WRF simulation.

b. CFD model

The CFD model domain ranges from 127°03′55.04″ to 127°04′59.0″E and from 37°31′57.9″ to 37°32′54.47″N. The horizontal grid interval is 10 m in the x and y direction, and the horizontal grid dimension is 180×180. In the vertical information of CFD model, a non-uniform grid system with 76 layers is employed, in which the vertical grid interval is uniform with 5m up to the 37th layer, increases with an expansion ratio of 1.1 from the 38th layer to the 52nd layer, and is then uniform with 20.89 m from the 53rd layer to the 76th layer. The time step used is 1 s.

Figure 2(a) represents a picture of Konkuk university area after high rise residential buildings are constructed. At the south-west direction of the model domain, high rise apartment complex and residential buildings are located. Likewise, it is very important to minimize damage from pollutants emitted by vehicles and buildings as population dense a limited space. Because pollutants are spread out surrounding areas in a short time by flow, it is requested to predict most of all.

Recently Geographical Information System (GIS) data which has height and position of buildings for 1 m interval is usable. It is essential using GIS data to predict urban environment because GIS data is used to make a topographical domain in a short time. Figure 2(b) shows building configuration in the CFD model domain. Interpolated model results are compared with observed values based

(a)

(b)

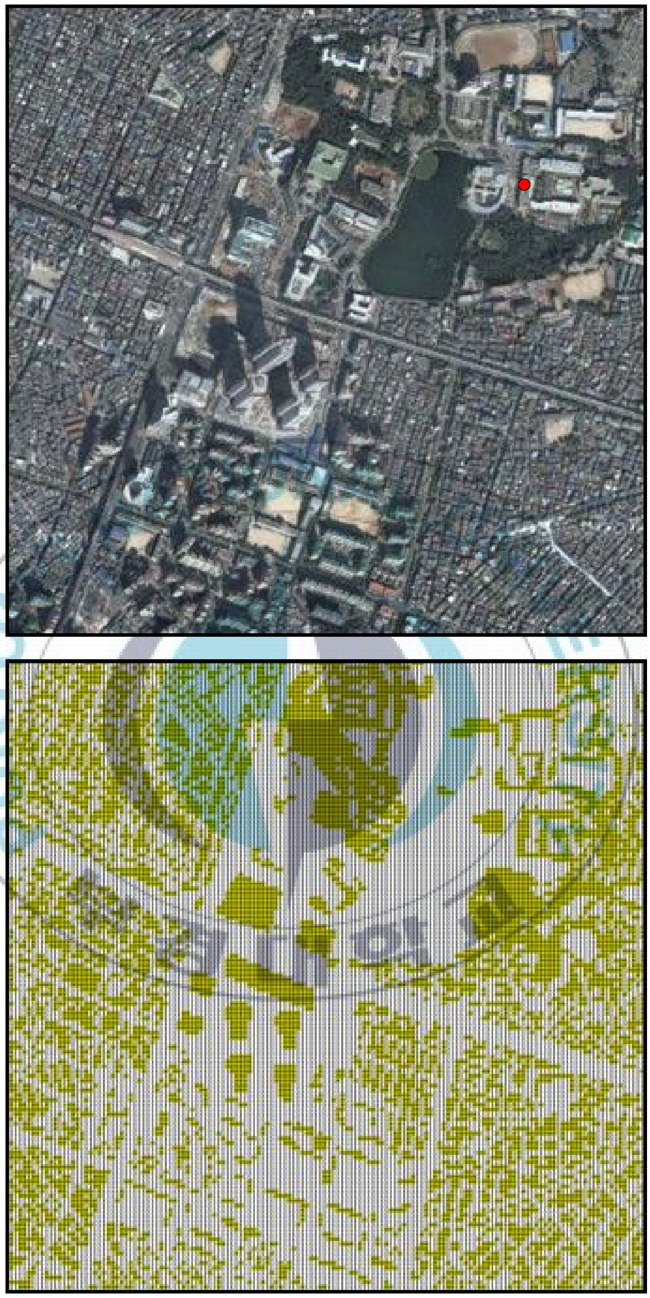

Fig. 2. (a) A picture of Konkuk university area and (b) building configuration in the CFD model domain.

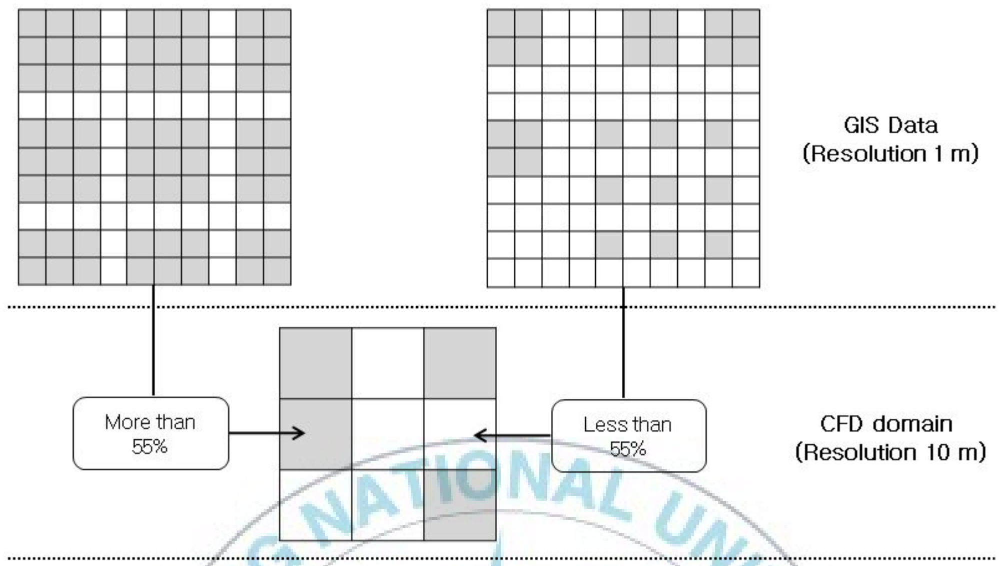

Fig. 3. The schematic process of constructing model domain for a CFD using a GIS data.

on a position of Kwangjin AWS located at marked a red color. Figure 3 shows the schematic process of constructing model domain for a CFD using a GIS data. To make a model domain including buildings and topography under limitation of a computing power, a model domain is downscaled ratio of 1:10. We also give an effort to minimize building effect which located outside of a computational domain (Fig. 4).

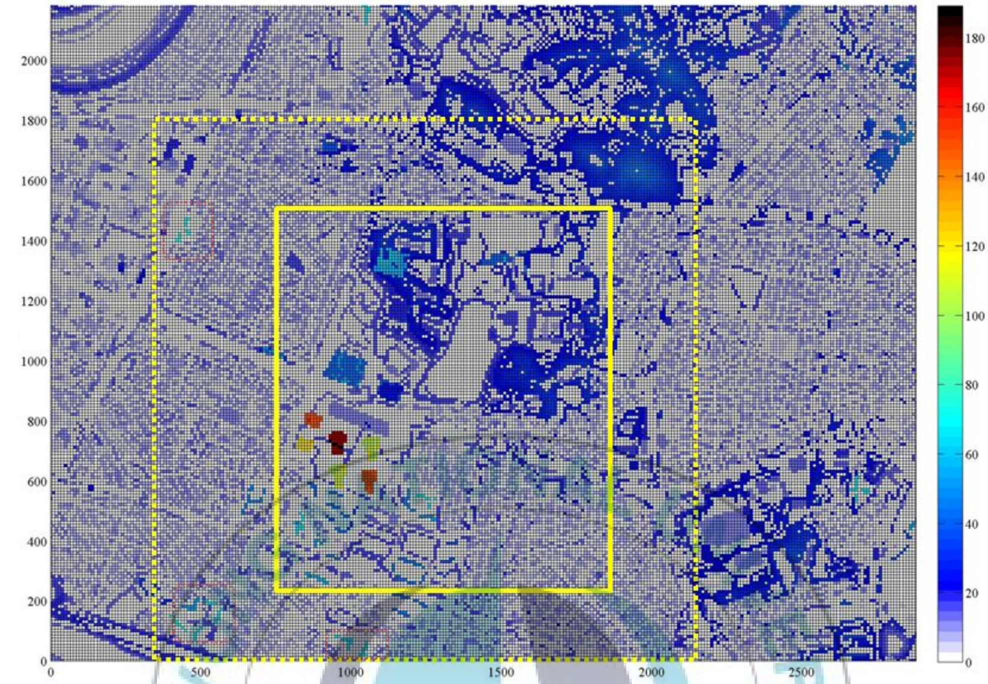

Fig. 4. Simulated area (yellow broken line) and interest area (yellow solid line)

2.4. Coupling method

In this study, u, v components and TKE data which obtained by a mesoscale model are used to initial and boundary conditions for the CFD model. Figure 5 represents the grid structure in WRF and CFD model domain which has same location of the center. There are nine grid cell from the WRF simulation are actually used for the CFD model simulation. It is noted that there are large differences in domain size and grid interval between the CFD and WRF model. The horizontal grid interval of the innermost WRF domain is 1 km, which is about the horizontal domain size of the CFD model. As the horizontal grid interval of the CFD domain is 10 m, nine grid cell information which have u, v components and TKE data should be integrated to define each grids of CFD domain. Two dimentional linear integration method to make a micro scale simulation domain is written as

$$e = \frac{W_4}{W_3 + W_4} x_1 + \frac{W_3}{W_3 + W_4} x_2 \tag{10}$$

In equation (10), x_1 and x_2 are obtained using values of a, b, c and d and equation (11) is used to carry out horizontal integration.

$$e = \frac{1}{(W_3 + W_4)(W_1 + W_2)} \{ W_3 (a W_2 + b W_1) + W_4 (c W_2 + d W_1) \} \qquad (11)$$

The vertical information of WRF model is from 50 m to 850m in order to include highest elevation in CFD model simulation. Therefore 17 simulated vertical layers are extracted from the WRF model. To provide grid information from WRF model simulation the linear interpolation is applied to horizontal and vertical direction. In the case of horizontal direction, simulated data from the WRF model is used from 50m to 840m in CFD model and wind profile power law with reference values of wind direction and speed in 50 m is employed below 50 m which elevation without the WRF model data due to the topographical effects.

$$\frac{U}{U_r} = (\frac{Z}{Z_r})^a \qquad (12)$$

Where a (=0.6) is a factor that is considered roughness effect in typical urban area.

For TKE, the linear interpolation method is employed using simulated data higher than 50 m and TKE is fixed below 50 m because it is difficult to predict unlike wind components which is possible to predict relatively accurately.

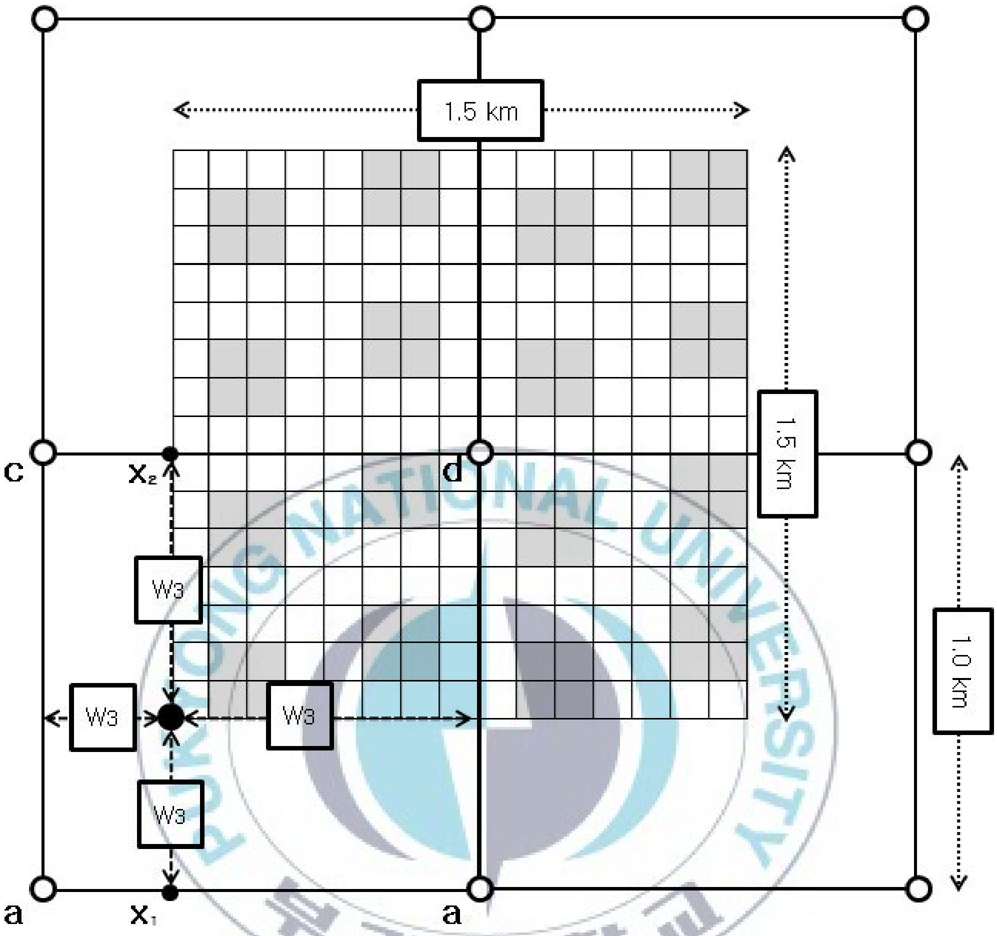

Fig. 5 The grid structure in WRF and CFD model

3. Results and discussion

3.1. Verification of a WRF model

In order to use simulated data with a WRF model for boundary conditions in a CFD model, the simulated synoptic weather extracted from the outmost domain is first compared to the observed whether which is well simulated. Figure 6 shows the WRF-simulated sea level pressure field at t = 6h after 6 hours for spin-up time and the observed one at the corresponding time (00 UTC 10 January 2009). At this time, the observed sea level pressure field exhibits a high-pressure system over in China and a low-pressure system right part of Japan. Most of isobars are split into small form in the whole area of China but there is almost no pressure difference near the Korean and Japan region. Moreover it shows a typical pressure system in winter. Thus these observed high- and low-pressure systems are well simulated using a WRF model. Figure 7 (a), (b) shows the WRF-simulated sea level pressure field at t = 30h (corresponding to 00 UTC 11 January 2009). Isobars near China also are split into many small pieces as it appeard at 00 UTC 10 January 2009. However movement and variation of pressure system during 24 hours is simulated well.

Wind direction and wind speed measured from Kwangjin Automatic Weather System (AWS) are compared with simulated data

(a)

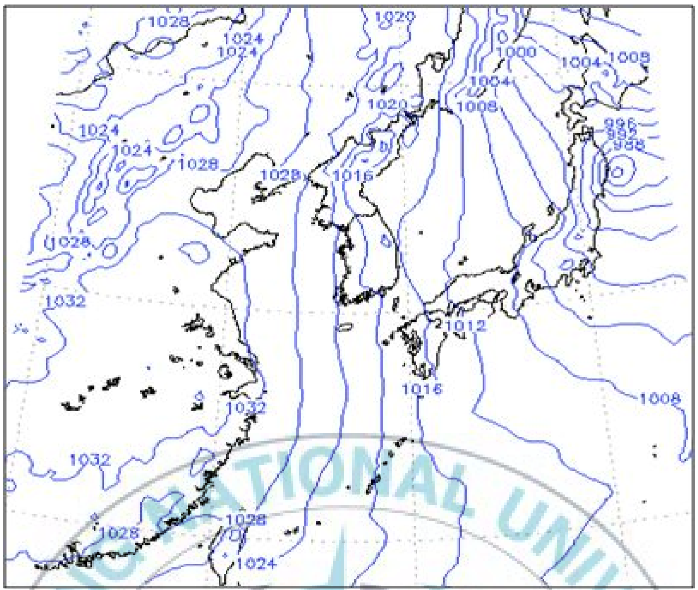

(b)

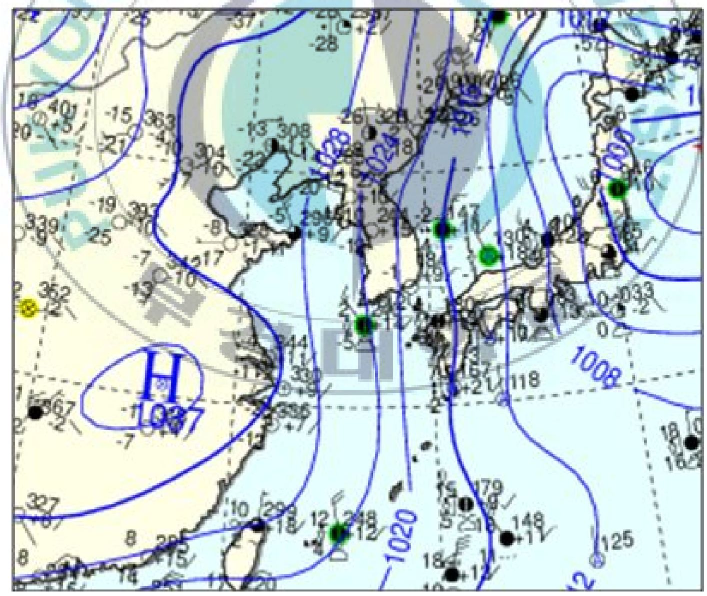

Fig. 6. (a) Simulated sea-level pressure field at 00 UTC 4 August 2006 and (b) Observed sea-level pressure field at 00 UTC 4 August 2006 from KMA weather chart.

(a)

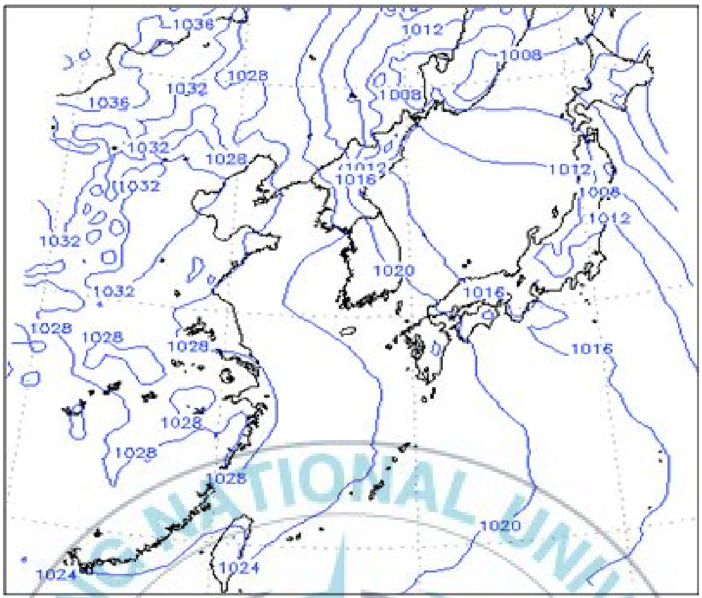

(b)

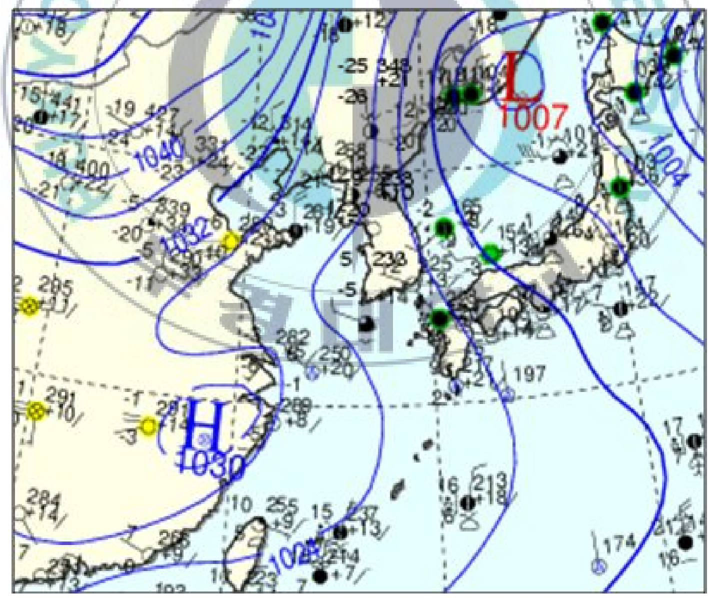

Fig 6. (a) Simulated sea-level pressure field at 00 UTC 5 August 2006 and (b) Observed sea-level pressure field at 00 UTC 5 August 2006 from KMA weather chart.

because the innermost area of WRF model simulation is used for initial and boundary conditions of CFD model. In the case of temperature data, it is not directly used in a coupled model but it is one of the factors which can affect on TKE. Therefore temperature also used for verification data. Observed data from Kwangjin AWS located at z = 52m is compared with simulated data extracted from same elevation in WRF model. Figure 8 represents time series of simulated and observed temperature at z = 52m in 10 minutes interval. The temperature simulated in a mesoscale model is 1.63℃ lower than observed one, but it shows general diurnal variation of temperature in winter by and large.

Figure 9 is a time series of simulated and observed wind direction at z = 52. Until t = 17h, a mesoscale model and a coupled model generally follow observed wind direction, but there is large differences after t = 17h. This reason is considered because as CFD domain scale is reduced, it can't product exact building obstacles.

It seems that there are some buildings which make a change of wind direction when it blows easterly.

Figure 10 shows a time series of simulated and observed wind speed at z = 52m. Two model simulations follow observed wind speed except parts of time. Especially, a coupled CFD-WRF model is more accurately predict wind speed than a WRF model alone.

Temperature, wind direction and speed which simulated using the WRF model is compared with observed data. There are some differences regarding a strength of each variable, but variation of time series as time varying show similar patterns and a coupled model improved strength of wind speed. Therefore it is decided that simulated data in a mesoscale model is possible to use in boundary conditions of a CFD model.

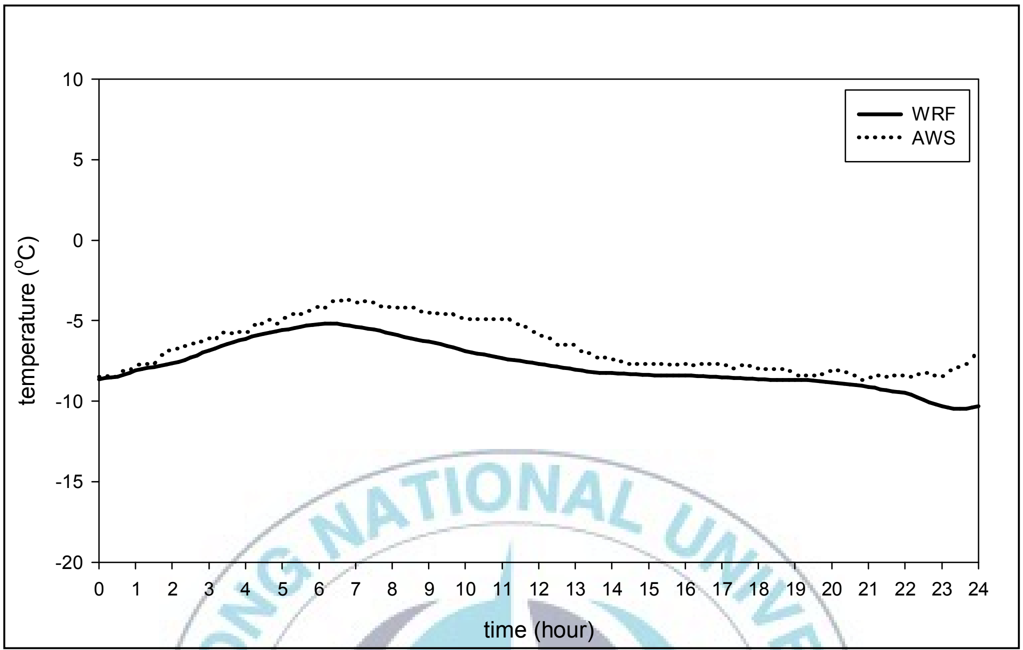

Fig. 8. Time series of simulated and observed temperature at z = 52m

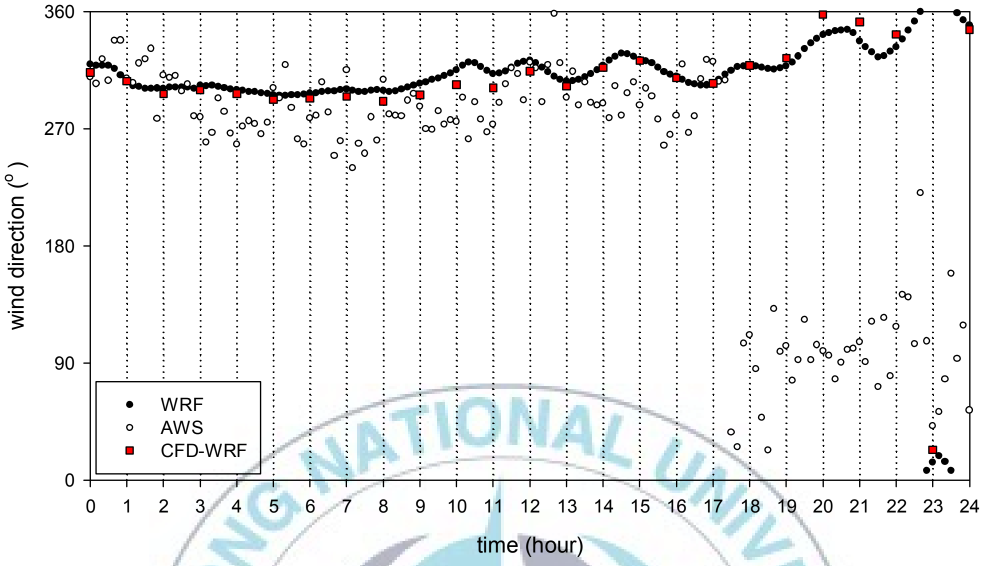

Fig. 9. Time series of simulated and observed wind direction at z = 52m.

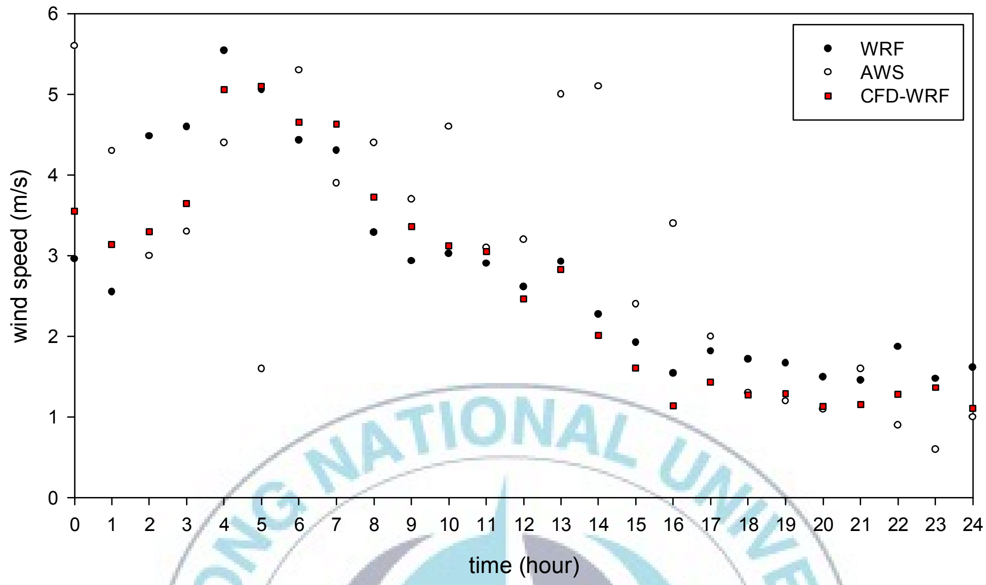

Fig. 10. Time series of simulated and observed wind speed at z = 52m.

3.2. Simulation with a coupled CFD-WRF model

The CFD model coupled to WRF is integrated for 30 hours starting from 18 UTC 9 January. Figure 11 shows time series of simulated wind direction using a WRF and a coupled CFD-WRF model and observed wind direction at z = 52m. It is observed from Fig. 11 that the result of a coupled CFD-WRF model shows considerably similar pattern in a WRF model simulation for most of the time. There is no interaction between synoptic and regional factor because the model used in this study is one-way coupled model. Therefore if influence by buildings are weak, result of a coupled CFD-WRF model is generally same as result of a WRF model because result data from a WRF model is used for initial and boundary conditions in a coupled model. Actually high rise buildings which affect flow pattern located at a enough distance from AWS and there is no obstacles to change flow rapidly. Thus it is confirm that Kwangjin AWS is located where it represent a synoptic wind for there region despite existence of many complex buildings.

Table 2 shows mean error and correlation of wind speeds simulated in WRF and CFD-WRF model to observed wind speeds in AWS. WRF model overestimated wind speeds but, the coupled CFD-WRF model underestimated -0.106 than AWS. It is because the coupled CFD-WRF model could reflect roughness effects by buildings or obstacles. Correlations between results of a numerical model and an observed one shows that the CFD-WRF model improved predicting wind speeds than WRF model alone.

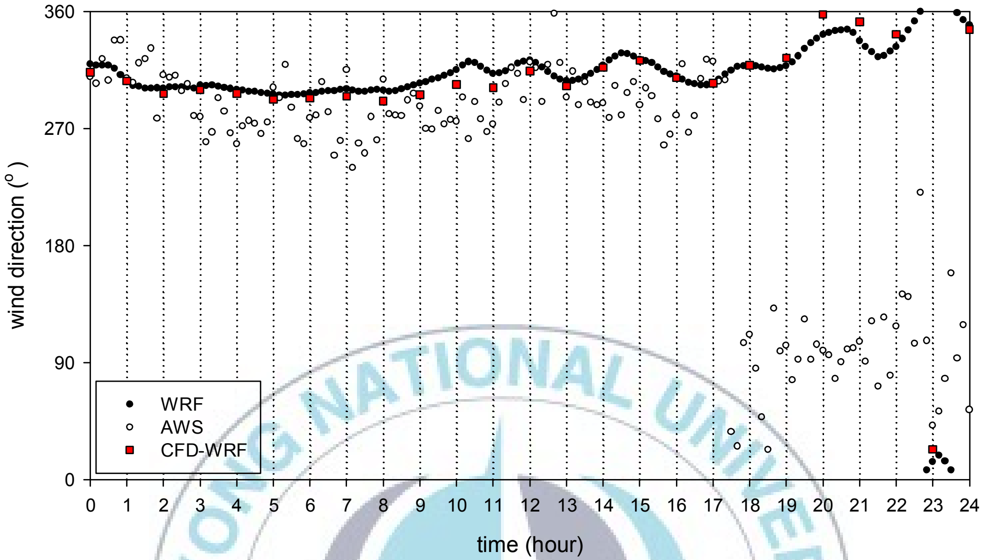

Fig. 11. Time series of simulated wind direction using a WRF and a coupled CFD-WRF model and observed wind direction at z = 52m.

Table 2. Mean error and correlation of wind speeds simulated in WRF and CFD-WRF model to observed wind speeds in AWS

	Mean error	Correlation
WRF vs AWS	0.055	0.368
CFD-WRF vs AWS	-0.106	0.526

4. Summary and conclusion

This study examined urban flow in a densely built-up area of Kwangjin in Seoul using a computational fluid dynamics model coupled to a mesoscale model (WRF). To provide initial and boundary condition for a CFD model, a mesoscale model (WRF) is used to simulate a flow in an urban area. Temperature, wind direction and wind speed which simulated using a WRF model and a coupled CFD-WRF are compared with observed data. On the basis of results from a WRF model which simulate regional circulation well, u, v wind component and turbulence kinetic energy are interpolated with a linear interpolation to make a boundary condition for a CFD model. Using a coupled CFD-WRF model, flow around Konkuk university is simulated for 30 hours from 18 UTC 9 January in 2009 with spin-up time for 6 hours. It was shown that the flow in the presence of real building clusters can change significantly as the ambient wind speed and direction change.

At the z = 2.5m next above the surface of model domain, inflow from the model boundary is changed variously due to the building effects. Wind speed is increased as flow converges between buildings. Moreover recirculation flow is made near buildings and double eddy circulation also appeared. These results suggest that time-dependent boundary conditions should be used to better predict urban flow using a CFD model and that a coupled CFD-mesoscale model can be reliably used for such a prediction.

However it is hard to verify model results with a single observed data. Therefore much more measured data is needed to predict flow in urban areas.

References

김재진. 2007: 장애물 외관비가 주변 흐름에 미치는 영향. *대기*, **17**, 381-391.

김재진, 백종진. 2005: CFD 모형을 이용한 도시 지역 흐름 및 스칼라 분산 연구. *한국기상학회지*, **41**, 821-837.

A.K.M. Chu, R.C.W. Kwok, K.N. Yu, 2005: Study of pollution dispersion in urban areas using Computational Fluid Dynamics (CFD) and Geographic Information System (GIS). *Environmental Modelling & Software.*, 20, 273-277

Baik, J.-J. and J.-J. Kim. 1999: A numerical study of flow and pollutant dispersion characteristics in urban street canyons. *J. Appl. Meteor.*, **38**, 1576-1589.

Baik, J.-J., R.-S. Park, H.-Y. Chun and J.-J. Kim. 2000: A laboratory model of urban street-canyon flows. *J. Appl. Meteor.*, **39**, 1592-1600.

Brown, M.J., R.E. Lawson Jr., D.S. DeCroix, and R.L. Lee. 2000: Mean flow and turbulence measurements around a 2-D array of buildings in a wind tunnel. *11th Joint Conference on the Applications of Air Pollution Meteorology with the A&WMA*, Long Beach, CA, U.S.A., 35-40.

Cheng, X., and F. Hu, 2005: Numerical studies on flow fields around buildings in an urban street canyon and cross-road. *Adv. Atmos. Sci.*, **22**, 290-299.

DePaul, F.T. and C.M. Sheih. 1986: Measurements of wind velocities in a street canyon. *Atmospheric Environment,* **20**, 455-459.

Kim, J.-J., and J.-J. Baik. 1999: A numerical study of thermal effects on flow and pollutant dispersion in urban street canyon. *J. Appl. Meteor.*, 38, 1249-1261.

Lee, I. Y. and H. M. Park. 1994: Parameterization of the pollutant transport and dispersion in urban street canyons. *Atmospheric Environment*, **28**, 2343-2349.

Liu, C.-H., and M. C. Barth, 2002: Large-eddy simulation of flow and scalar transport in a modeled street canyon. *J. Appl. Meteor.*, **41**, 660-673.

Meroney, R.N., M. Pavageau, S. Rafailidis and M. Schatzmann. 1996: Study of line source characteristics for 2-D physical modelling of pollutant dispersion in street canyon. *Journal of Wind Enginnering and Industrial Aerodynamics*, **62**, 37-56

Nakamura, Y. and T.R. Oke. 1988: Wind, temperature, and stability conditions in an east-west oriented urban canyon. *Atmospheric Environment*, **22**, 2691-2700.

Rotach, M.W. 1995: Profiles of turbulence statistics in and above an urban street canyon. Atmospheric Environment, **29**, 1473-1486.

Sini, J.-F., S. Anquetin, and P.G. Mestayer. 1996: Pollutant dispersion and thermal effects in urban street canyons. *Atmospheric Environment*, **30**, 2659-2677.

Uehara, k., S. Murakami, S. Oikawa and S. Wakamatsu. 2000: Wind tunnel experiments on how thermal stratification affects flow in and above urban street canyons. *Atmospheric Environment*, **34**, 1553-1562.